

# REPORT OF THE MICROVERTEX DETECTOR GROUP

T. Kondo

KEK, National Laboratory for High Energy Physics  
Oho-machi, Tsukuba-gun, Ibaraki-ken, 305 JAPAN

Bruce Barnett	Johns Hopkins University	Randy Ruchti	University of Notre Dame
David Berley	National Science Foundation	Paul Shepard	University of Pittsburgh
Lucien Cremaldi	University of Colorado	Jean Slaughter	Fermilab
Erik Heijne	CERN	Darrel Smith	University of California, Riverside
Kenneth Heller	University of Minnesota	Toshiaki Tauchi	KEK
Harris Kagan	Ohio State University	George Theodosiou	University of Pennsylvania
Jean Pierre Merlo	CERN	George Trilling	Lawrence Berkeley Laboratory
Lawrence Price	Argonne National Laboratory	Michal Turala	University of California, Santa Cruz

## 1. SUMMARY

The Microvertex Detector Working Group tried to address the two major questions:

1. Can microvertex detectors be built for the SSC that will be able to work under the severe environmental requirements of  $\sqrt{s} = 40$  TeV and  $L = 10^{33}/\text{cm}^2/\text{sec}$ ?
2. What are their expected performances in detecting secondary vertices?

In order to answer these questions, we have concentrated our effort on a specific design based on silicon microstrip detectors. In addition we performed Monte Carlo simulations of high  $P_T$  events to evaluate how bad (dirty) the situation at around the interaction point is for detecting any secondary vertices. We have concentrated our study only in the central rapidity region ( $|y| < 2$ ), since the situation at the forward and backward regions is so different from that of the central region that an entirely new detection concept has to be applied.

## 2. ROLES OF MICROVERTEX DETECTORS

The principal role of microvertex detectors is to find secondary vertices. Existence of secondary vertices is one of the most powerful identifications of c or b quark jets or  $\tau$  leptons. Most of new physics expected at the SSC are something to do with W, Z, Higgs, heavy quarks and heavy leptons. W and Z frequently decay into  $\tau$  leptons, c and b quarks. Higgs, heavy quarks and heavy leptons often end up with b and c quark jets in their final states. Therefore detection of secondary vertices will greatly help the identification of these heavy particles together with other identification methods such as lepton tagging, jet invariant mass.

It should be mentioned that the role of the vertex detectors currently used in various  $e^-e^+$  colliding beam experiments is to measure the impact parameters of leptons and/or hadrons in the enriched event samples in order to statistically measure the lifetimes of B, D mesons and  $\tau$  leptons. This is no use for the SSC. The function of the microvertex detectors we presently aim is much harder, namely to find secondary vertices and use it as tagging or identification of c,b or  $\tau$  jets event by event.

There are additional important advantages to equip microvertex detectors for the SSC experiments :

- (1) better separation of multiple interactions within the same bunch crossing,
- (2) improvement of momentum resolution as well as pattern recognition capability.

At the luminosity of  $10^{33}/\text{cm}^2/\text{sec}$  and with bunch crossing every 15nsec, 44%(7%) of bunch crossing contains more than one(three) inelastic collisions. The most effective way of identifying such multiple interactions in the same bucket is to identify multiple interaction origins along z(beam) axis through charged particle tracking. The closer the detector to the beam pipe, the better the z reconstruction becomes.

As for the momentum resolution, the central tracking group concluded that it is impossible to place any type of wire tracking devices at smaller radius than 50 cm because of the occupancy problem at  $L=10^{33}/\text{cm}^2/\text{sec}$ . If one manages to operate a microvertex detector at the vicinity of the beam pipe, one could improve the momentum resolution by substantial amount and accordingly we can possibly shrink the outer radius of central tracking system (say by 50 cm), saving quite a number of wires plus their associated electronics as well as shrinking the entire volume of calorimeters, magnet, and muon detectors.

### 3. PERFORMANCE CRITERIA OF MICROVERTEX DETECTORS

As has been repeatedly pointed out<sup>1,2</sup>, the location for the detectors is the worst place one could think of for charged particle detection, namely at  $L = 10^{33}/\text{cm}^2/\text{sec}$  and  $\sqrt{s} = 40 \text{ TeV}$ :

charged particle flux:  $3 \times 10^6/\text{cm}^2/\text{sec}$  at  $r_T = 5 \text{ cm}$   
 radiation dose:  $10^6 \text{ rad/year}$

This is illustrated in Fig.1. The flux is based on the extrapolated minimum bias interactions with 6 charged particles per unit rapidity. The rate drops quadratically as transverse radius  $r_T$  from the beam pipe. It is obvious that any microvertex detector must have a extremely high rate capability together with high radiation resistance up to over 1Mrads.

In addition to the above high rate environments, one encounters the very high charged track density for high  $p_T$  events:

track density:  $\approx 500$  charged particles/event  
 collimated jets/decays:  $\theta_{op} \approx 20 \text{ mrad}$ .

This situation can be illustrated in Fig.2 in which all charged paricles of a Monte Carlo event with  $p_T = 2000 \text{ GeV}/c$   $b\bar{b}$  jets are displayed<sup>3</sup>. One sees a group of highly collimated particles coming from  $b$  quark jets. It is apparent that any detector must be highly segmented with a superb two track separation capability.

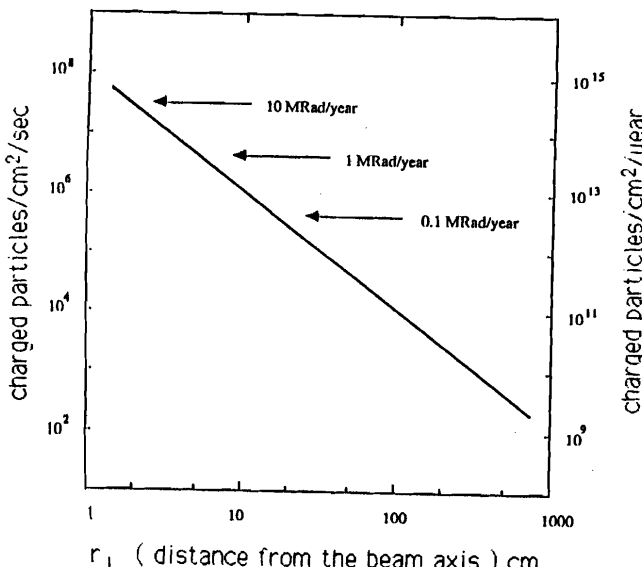


Fig.1 Charged particle rate at  $L = 10^{33}/\text{cm}^2/\text{sec}$  and yearly dose.

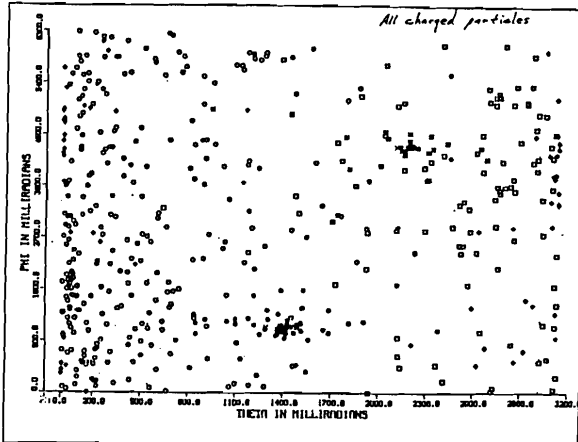


Fig.2 Charged particles generated in a Monte Carlo event with  $p_T = 2000 \text{ GeV}/c$   $b\bar{b}$  jets.

### 4. SIGNIFICANT TECHNICAL PROGRESS

At the time of 1984 Snowmass Study, we are very skeptical of the feasibility of any microvertex detectors<sup>1</sup>. The main reason was radiation damages of detectors as well as associated electronics. In addition, nobody has a confidence on readout of  $>>100K$  channels from narrow spaces to outside world. We have recognized that there have been several significant technical progress in last two years as digested in the followings:

#### (1) Custom integrated circuits for silicon strip detectors

SLAC/Hawaii/CERN group successfully developed a sampling & hold readout chip (Microplex) for silicon microstrip readout using NMOS technology. Various beam tests have been performed resulting S/N ratios of 15 for minimum ionizing particles<sup>4</sup>. As shown in Fig.3, it is demonstrated that, with strip detectors of  $25\mu\text{m}$  pitches, the position resolution can be less than  $5 \mu\text{m}$  and two track separation can be done down to  $150\mu\text{m}$  separation without any resolution losses<sup>5</sup>.

Encouraged by the success of the Microplex readout chips, several attempts have been initiated for better and low power versions of microstrip readouts of CMOS amplifiers ( MPI/Munich/Dortmund ), CMOS version of Microplex chips ( Rutherford ), S/H chips with sparse readout ( LBL/CDF ), PISO MOSCCD ( CERN/Phillips ), JCCD ( KEK/Hamamatsu ) e.t.c.

#### (2) Application of silicon detectors to colliding beam experiments

Encouraged with the remarkable successes of use of silicon microstrip detectors in many fixed targets<sup>6</sup>, physicists are seriously planning to integrate the same type of detectors into the big colliding beam detectors such as UA2, CDF, upgraded-Mark II and Delphi. Most of them are going to use specially developed readout microelectronics such as  $\mu$ -plexes.

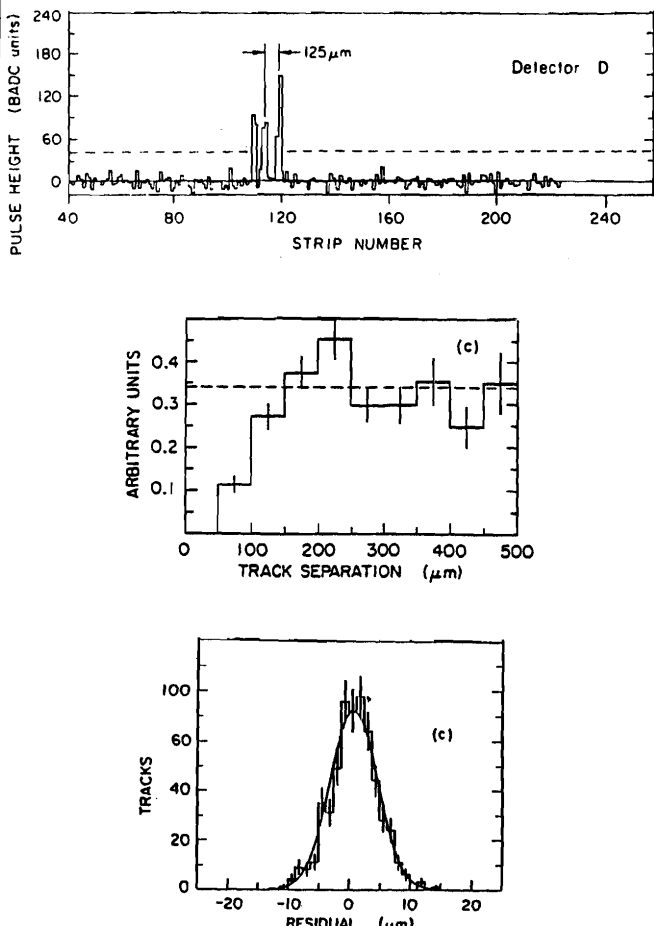


Fig.3 Results of SLAC beam test using  $\mu$ -plex chips.

TOP : A display of the corrected strip pulse height vs. strip number for a single 3 track event,  
 MIDDLE : Histogram of two track events as a function of two track separation,  
 BOTTOM : Position resolution.

### (3) Radiation hardness of electronics

Readout electronics of microvertex detectors such as preamplifiers and time slicing buffers have to be directly mounted to the detectors to solve the cabling problems. Therefore these electronic parts receive a fair amount of charged particle radiation, say over 1 Mrads in one year operation. The  $\mu$ -plex circuits are tested under  $\gamma$ -ray radiation and they failed at  $<10^5$  rad. However, it becomes clear that, for military use as well as for space and nuclear plant application, there have been many basic and practical researches of radiation hardening for many years<sup>7</sup>. Radiation hardened devices can stand up against over 1 Mrads, but the radiation resistivity critically depends on type of radiation, materials, circuit types, processing and so on. Therefore in principle there are hardening techniques available for use, but practically more R&Ds are needed especially low-noise, high-speed and low-power electronics.

### (4) Radiation damage tests of silicon strip detectors

Several basic tests have been performed using  $\gamma$ -rays and particle beams<sup>8</sup>. In general, ion-implanted pn-junction silicon detectors are most radiation resistant and can survive to  $10^{14}$  particles/cm<sup>2</sup>. Typically one observes an increase of reverse leak current due to radiation, but the leak current could be reduced by simply cooling the devices.

### (5) Scintillation fibers

A cerium based scintillation fiber glass (GS1/SC20) is successfully fabricated and tested with a hit density of 4.1/mm, much better than before<sup>9</sup>. However the attenuation length is estimated to be a few cm, still too short for colliding-beam detectors. Many new scintillation glass fibers have been proposed for further study<sup>10</sup>. An electronic readout system has been built and tested<sup>9</sup>.

### (6) Silicon Drift Chambers

A novel idea of silicon drift chamber has been proposed by Gatti and Rehak. They achieved  $\sigma=11\mu\text{m}$  with two dimensional resolution of  $20\mu\text{m}$  in a beam test<sup>11</sup>.

In summary, there are rapid technical progress going on in the field of semiconductor detectors and associated electronics. Expecting that this tendency will continue for a few more years, we can be rather optimistic about the feasibility of microvertex detectors for the SSC.

## 5. CHOICE OF DETECTOR TYPES

There are many possible types of detectors which could be applicable for high precision vertex detection :

- wire chambers
- scintillating fibers
- silicon microstrip detectors
- CCD or pixel devices
- silicon drift chambers
- superconducting junction devices

The last one is too new and primitive to be seriously discussed here.

At the luminosity of  $10^{33}/\text{cm}^2/\text{sec}$ , we think there remains little possibility left for any types of vertex wire chambers because of rate and occupancy problems<sup>2</sup>. Suppose we place the newly developed modular multicell drift chambers<sup>12</sup> with 1mm drift distance and 50cm in wire length at the radius of 10cm. The hit rate due to minimum bias events then becomes 10MHz, too high for any reasonable operation.

Small diameter scintillating glass fibers have been successfully made using Cerium based glass<sup>9</sup>. Its resistance to radiation is demonstrated to be good over  $10^6$  rad. It will be an interesting alternative but, at this

stage, the technique is still in its primitive stage and more R&Ds have to be performed for realistic proposal of any vertex detectors<sup>13</sup>. Among others, there need clever and realistic ideas for compact optical readouts.

CCD or pixel devices as well as silicon drift chambers are potentially very interesting devices for vertex detections. Besides being high precision detectors, they have superior capabilities for the pattern recognition of charged particles in comparison with other one dimensional devices. Thus, they are very attractive for the SSC since most of events will be quite complex. However, it is too primitive to say that we will be able to construct a microvertex detector from CCD, pixels or silicon drift chambers alone. They might be very useful if they are used in combination with other high precision devices. No useful information is yet available about their radiation damages.

We picked up silicon microstrip detectors mainly because they have been successfully used already in many fixed target experiments and therefore we think, expecting continuing technical progress, silicon microstrip detectors have the highest potentiality for a SSC microvertex detector.

## 6. DESIGN OF A SILICON MICROVERTEX DETECTOR

Fig.4 shows a schematic view of silicon microstrip detector and readout electronics. As we believe that use of high resistive wafers with 4" in diameter will soon be popular, silicon microstrip detectors of 9cm(L)×3.5cm(W)×0.02cm(T) are assumed. In addition, although not technically established so far, we require readout strips on both faces (junction and HV sides) forming large (or small) angle stereos in order to save the total radiation length. In the case of large angle (say 90°) stereo, several strips have to be combined for readout as shown in Fig.5.

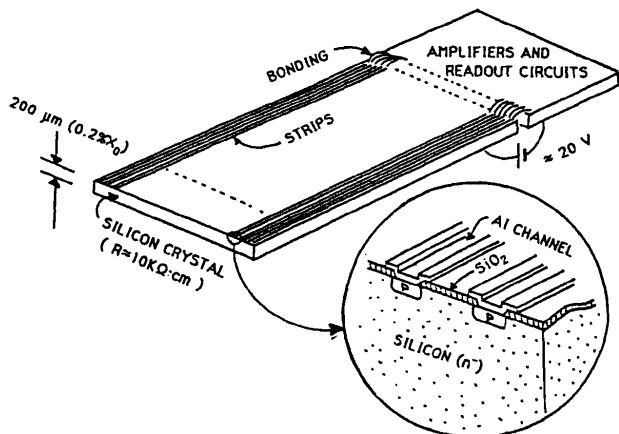


Fig.4 A sketch of silicon microstrip detectors.

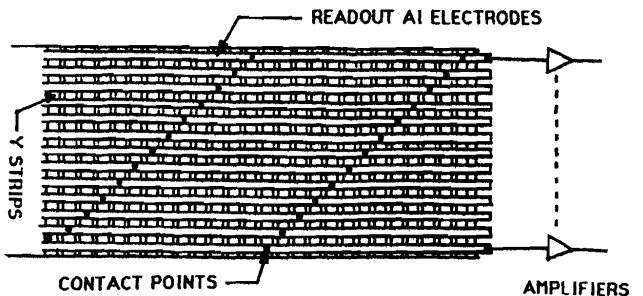


Fig.5 Stereo readouts of microstrip detectors.

As for their readout electronics, a simple sample and hold scheme used in for example  $\mu$ -plex chips does not work for the SSC because of the bunch crossing rate of 60MHz. What we need is a time slice buffering structure to temporally store information locally for say 1μsec. Readout to outside world is initiated after an event trigger is established. In addition, serial-parallel conversion must be performed at the detector end in order to save readout cables. An example, a PISO (parallel-in serial-out) analog buffer<sup>14</sup>, for silicon microstrip detectors is shown in Fig.6.

To form a microvertex detector, we tentatively assume five detector layers surrounding the beam pipe as shown in Fig.7. Five layers might not be enough to do a complete track pattern recognition by themselves for a complex event, but probably enough to perform the search and finding of track segments based on the extrapolated trajectories from the main tracking device. If we assume rms position resolution of 10μm and a detector to detector alignment of the same order, one obtains angular resolution of  $\approx 0.45\text{mrad}$  and impact parameter of an order of 45μm based on the measurement errors only.

The effect of multiple coulomb scattering in the beam pipe and the detectors is roughly estimated to be

$$\delta_b(\text{MS})^2 \approx (0.015/p)^2 \times \{(l \times \sqrt{t})^2_{\text{beam pipe}} + (l \times \sqrt{t})^2_{\text{detector}}\} \\ \approx \{(30\text{μm})^2 + (150\text{μm})^2\} / p^2$$

where  $p$  is the momentum in GeV/c,  $l$  is the distance from the interaction point and  $t$  is the radiation length. We assume  $t = 0.005$  and  $0.004$  for the beam pipe and each detector plane, respectively. Combining these two resolutions one gets

$$\delta_b \approx \sqrt{(155\text{ μm}/p)^2 + (45\text{ μm})^2}.$$

We notice that, below 4 GeV/c, the multiple Coulomb scattering (especially in the detectors) is the dominant error source of vertex resolution. The impact parameter

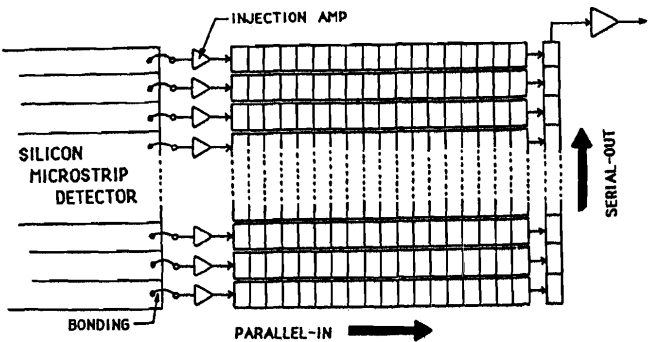


Fig.6 Parallel-in serial-out (PISO) readout.

resolution thus obtained is compared with the maximum impact parameters generated by D or B particle decays,

$$\delta_b(\text{decays})_{\text{MAX}} \approx c\tau \approx 3 \times 10^{10} \times 10^{-12} = 300 \text{ } \mu\text{m}.$$

Typical impact parameters are somewhat smaller than this value due to decay kinematics and mass effects. In conclusion, we see that the impact parameter resolution is enough for the case say above 10 GeV/c or so. This will be demonstrated in our crude Monte Carlo simulation described in the following section.

Table 1 summarizes our tentative design of the microvertex detector. It should be noted that there are no occupancy or rate problems because of the extremely fine segmentation. However we ended up with a huge number of readout channels, i.e. close to 1 million readout channels! We have assumed preamplifiers with PISO readout buffers directly mounted somehow onto the detector. If we optimistically assume the power consumption of 2 mW per channel, the total power dissipation at the detector is  $\approx 2 \text{ KW}$  for such a narrow space. A very clever way of heat cooling is necessary.

It is pointed out that nuclear interactions and photon conversions in the beam pipe and in microstrip detectors might fake seriously the secondary vertices. The total radiation length and nuclear collision length is optimistically estimated to be 2.5% and 0.8% respectively. Photon conversions introduce negligible transverse kicks and thus do not harm for vertex finding. Nuclear interactions make a nuisance to secondary vertex detection. Hopefully a momentum cut will greatly suppress such backgrounds.

Table 1. A Design of SSC Microvertex Detector.

detector element	silicon microstrip detector with double sided strips				
detector size (L×W×T)	9cm × 3.5cm × 0.02cm				
strip pitch	25 or 50 $\mu\text{m}$				
total number of detectors	494				
total number of strips	920K				
total radiation thickness	2 %				
readout electronics	parallel-in serial-out buffers attached to detectors				
readout speed	60 MHz for event buffering 1 MHz for serial readout				
total number of readout	934K				
total power dissipation	2 KW (?)				
layer number	1	2	3	4	5
detector radius	5	7.5	10	12.5	15 cm
strip pitch	25	25	25	50	50 $\mu\text{m}$
number of strips	75K	157K	252K	185K	265K
radiation dose	1	0.4	0.25	0.16	0.1 Mrad/yr
hit rate/strip	64	32	19	26	18 KHz
occupancy(M.B.)	0.6	0.3	0.2	0.3	0.2 %
occupancy(high $p_T$ )	1.3	0.7	0.4	0.5	0.4 %

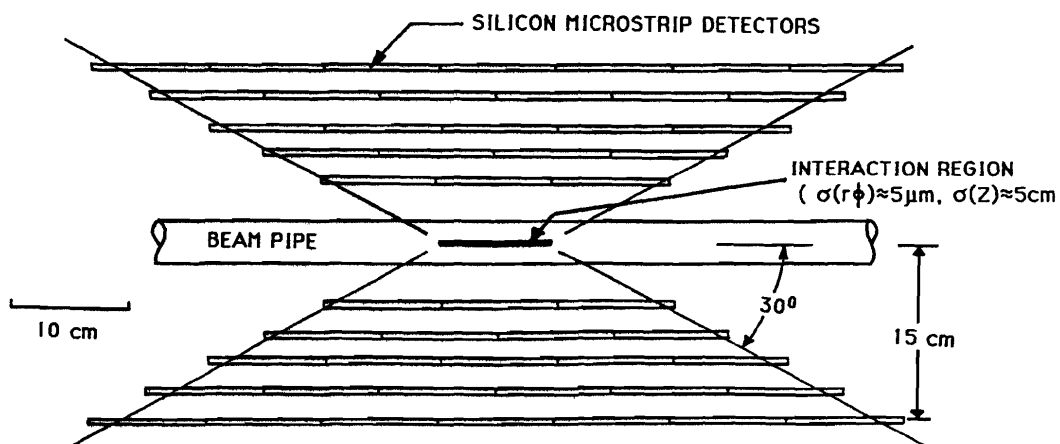


Fig.7 Schematic view of a microvertex detector.

## 7. MONTE CARLO EVENT SIMULATIONS

During the summer study, we have performed several Monte Carlo simulations in order to get feelings of the tracking situation at around the interaction point.

Among others, one of the simple simulation programs developed by T.Tauchi was successfully completed during the summer study. The program is based on the event generation program ISAJET V5.23 with additional capability of secondary vertex generation for B and D mesons. An axial magnetic field of 1.5 Tesla is assumed in the program. Though any detector configurations can be set in the program, the detector geometries are fixed to those given in Table 1 for the present study. The program, not only traces the charged particle trajectories through the detectors including the multiple Coulomb scattering effects, but also performs the circle fitting to get the reconstructed impact parameters in the  $r\phi$  plane taking the detector digitization (25 $\mu$ m/50 $\mu$ m) into account.

In the present simulation, for simplification, only one type of high  $p_T$  QCD jet events,  $p+p \rightarrow b+\bar{b}+X$ , are generated at  $\sqrt{s} = 40$  TeV,  $p_T = 500$  GeV/c and  $\theta = 90^\circ$ . Details of the present simulation is summarized in Table 2.

Table 2. Monte Carlo Simulation

Generation program	ISAJET V5.23
Events generated	$p+p \rightarrow b+\bar{b}+X$ (QCD process)
$p_T$ of $b, \bar{b}$ jets	500 GeV/c
$\eta$ of $b, \bar{b}$ jets	0 ( $\theta = 90^\circ$ )
$\tau(B^{0,\pm}), \tau(D^0), \tau(D^\pm)$	$(1.4, 0.44, 0.92) \times 10^{-12}$ sec
Detector configuration	as Table 1 and Fig. 7 (but no divisions of strips in the Z direction)
Magnetic field	1.5 Tesla axial
No. of events generated	100
Tracks traced	$30^\circ < \theta < 150^\circ$
Multiple scattering	ON (2mm Be beam pipe, 400 $\mu$ m thick each Si plane)
Track reconstruction	circle fit in $r\phi$ plane

Fig.8 shows the  $r\phi$  view of several typical events with the detector arranged as proposed above. Charged particles from B and D decays are denoted by solid and broken lines, respectively. One sees quite many charged particle tracks (165 on average in  $30^\circ < \theta < 150^\circ$ ) emerging from the primary vertex point. However the magnified views shown in the right indicate that the tracks are not so crowded in the scale of the strip width of 25 or 50 $\mu$ m. One also notices that the opening angles of B or D decays are quite small ( $\approx 10$  mrad) due to high energy nature as expected.

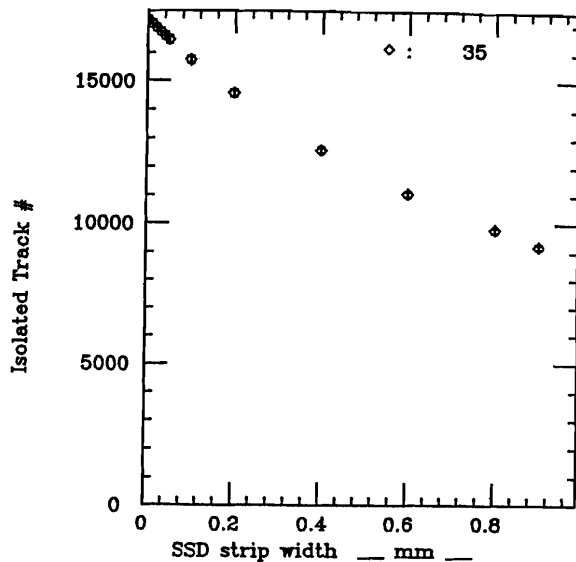


Fig.9 Number of isolated hits observed as a function of strip width at  $r=5$  cm.

The track-to-track separation at the first layer of the microvertex detector ( $r=5$  cm) is shown in Fig.9. The figure indicates that two track separation of much less than 1 mm is essential at radius 5 cm in order to keep the tracking efficiency high. The proposed microstrip system with possible two track separation of 150 $\mu$ m would be well matched with this requirement.

As shown in Fig.10, the typical decay length of B mesons is Lorentz boosted to an order of 1 cm as expected. Therefore sometimes, but not so often, the decay points locate in the detector area.

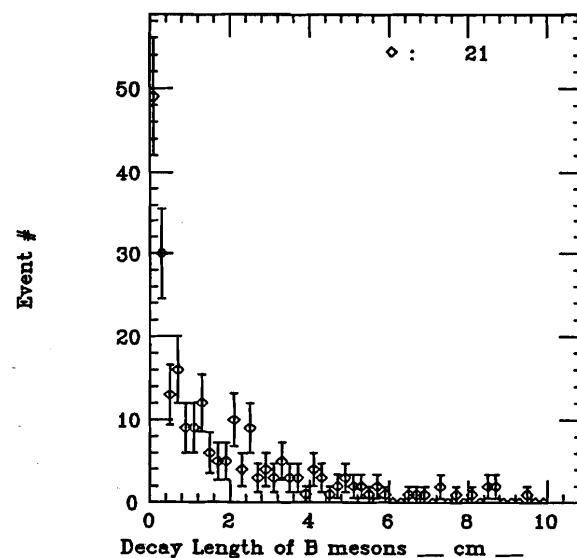
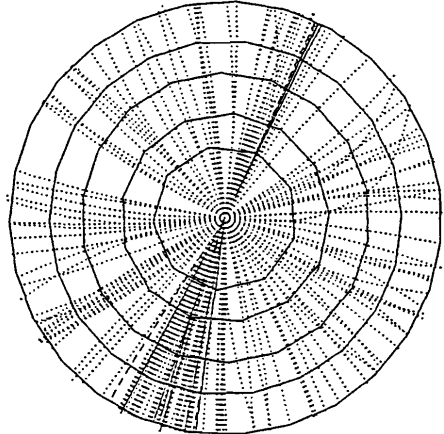
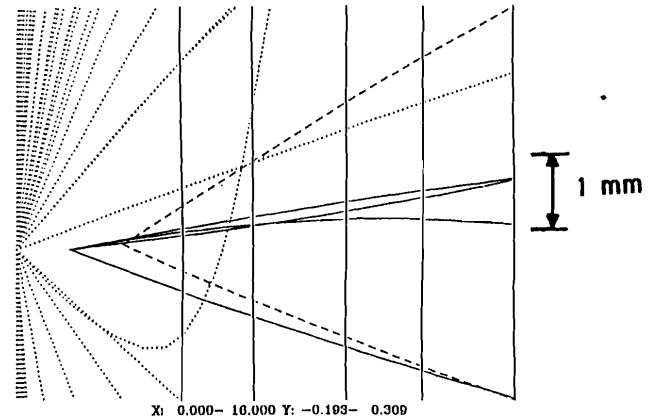


Fig.10 Decay length distribution of B meson decays.

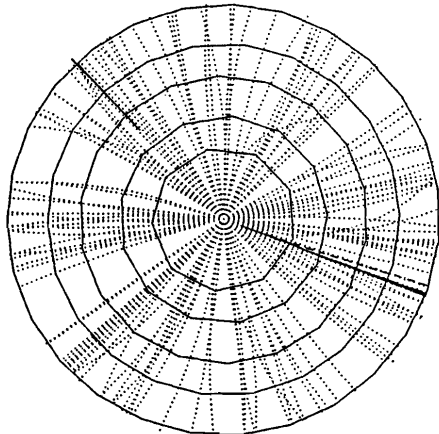
One Event Display in SSD \*\*\* EVENT#= 39  
TWOJET : P +P ->BT +BB PT=500.GEV ECM=40.0 TEV



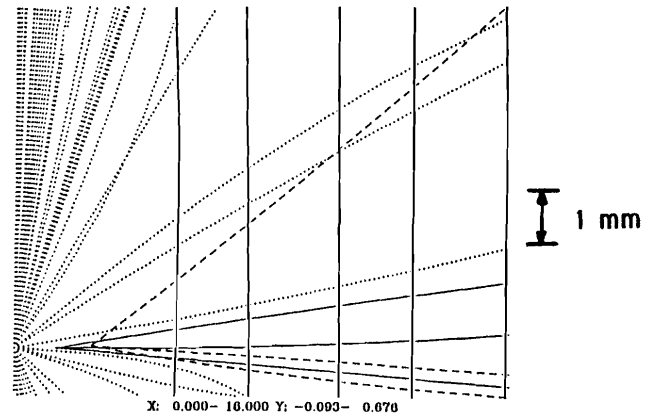
One Event Display in SSD \*\*\* EVENT#= 39  
TWOJET : P +P ->BT +BB PT=500.GEV ECM= 40.0 TEV



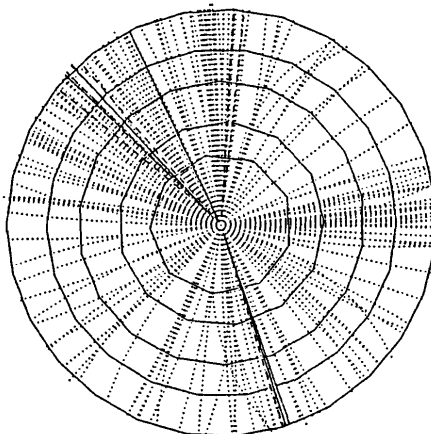
One Event Display in SSD \*\*\* EVENT#= 56  
TWOJET : P +P ->BT +BB PT=500.GEV ECM=40.0 TEV



One Event Display in SSD \*\*\* EVENT#= 56  
TWOJET : P +P ->BT +BB PT=500.GEV ECM= 40.0 TEV



One Event Display in SSD \*\*\* EVENT#= 89  
TWOJET : P +P ->BT +BB PT=500.GEV ECM=40.0 TEV



One Event Display in SSD \*\*\* EVENT#= 89  
TWOJET : P +P ->BT +BB PT=500.GEV ECM= 40.0 TEV

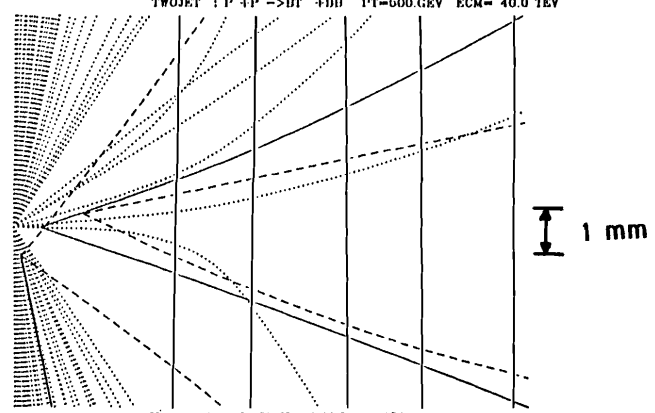


Fig.8 Typical  $b\bar{b}$  events with  $p_T=500\text{GeV}/c$  at  $\sqrt{s}=40\text{TeV}$  at  $\theta=90^\circ$ . Projected trajectories of charged particles with  $30^\circ < \theta < 150^\circ$  are shown with dotted lines in the  $r-\phi$  projected plane. The silicon microstrip detectors assumed are indicated by solid lines. Charged particles from  $B$  ( $D$ ) decays are shown with solid (broken) lines. Pictures in the right are enlarged (in  $\phi$  direction) view of the vicinity of one of the secondary vertices.

Now, in order to see how good we can identify the secondary vertices, a simple circle fitting program is used for track reconstruction in the  $r$ - $\phi$  projected plane (but skipping the pattern recognition procedures). The reconstructed impact parameter  $b_r$  is obtained for each track. Two dimensional plots in Figs.11-a and 11-b separately show the distribution on the  $b_r$ - $p_T$  plane for the tracks coming from the primary and secondary vertices, respectively. There we see a clear difference in the reconstructed impact parameters well above the spreads in  $b_r$  coming from the multiple scattering and the detector resolution. Then we introduce a very primitive cut on  $b_r$  and  $p_T$  to obtain the efficiency and S/N ratio for the identification of the tracks from secondary vertices. The results are summarized in Table 3 and Fig.12. The S/N ratio of  $>20$  can be obtained while keeping the finding efficiency for tracks from secondary vertices  $>50\%$  with suitable  $b_r$  and  $p_T$  cuts as far as 500GeV/c  $b\bar{b}$  events concern. This is quite encouraging.

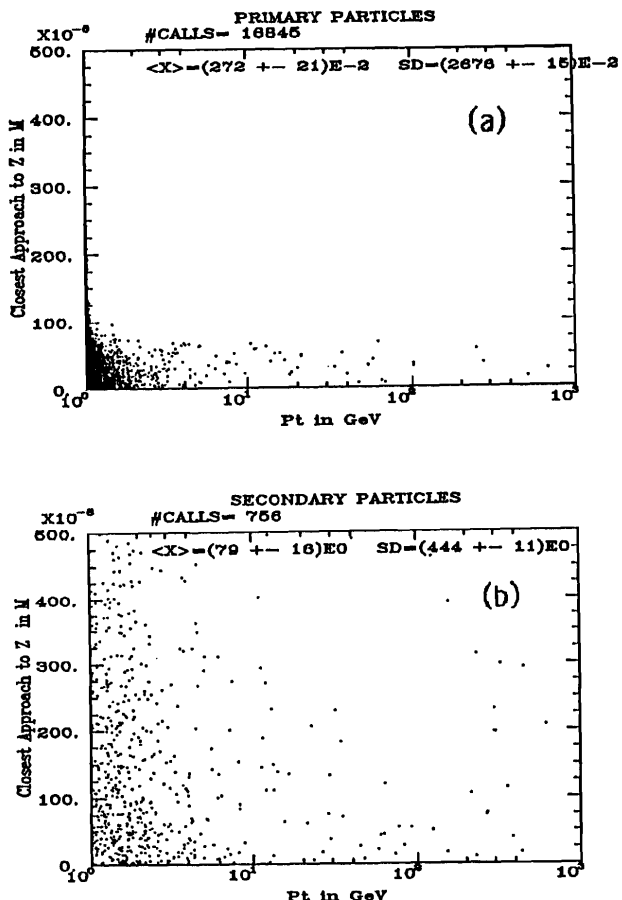


Fig.11 Reconstructed impact parameter  $b_r$  vs  $p_T$  for charged particles (a) from the primary vertex and (b) from the secondary vertices.

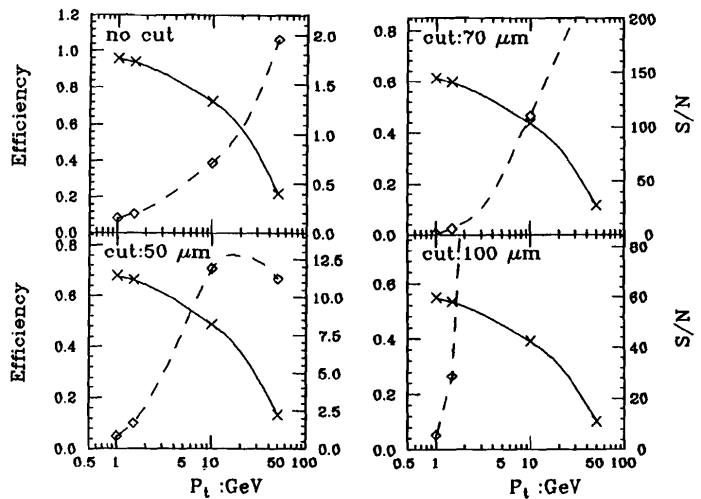


Fig.12 The efficiency (x, —) and S/N ratio (diamond, ---) for finding secondary vertices by impact parameter cuts in the  $r$ - $\phi$  plane as a function of  $p_T$ .

Table 3. Summary on reconstructed 100  $b\bar{b}$  events with  $p_T = 500$  GeV/c

$p_T$ cut (GeV/c)	$b_r$ cut ( $\mu\text{m}$ )	primary tracks	secondary tracks	S/N	efficiency (%)
>1.0	non	16845	756	0.04	100
	> 50	8552	539	0.06	71
	> 70	7144	489	0.07	65
	>100	5683	438	0.08	58
>1.5	non	4868	725	0.15	96
	> 50	600	513	0.86	68
	> 70	243	464	1.91	62
	>100	74	414	5.59	55
>10.	non	3661	711	0.19	94
	> 50	295	501	1.69	66
	> 70	79	453	5.73	60
	>100	14	404	28.9	53
>50.	non	765	548	0.72	72
	> 50	31	370	11.9	49
	> 70	3	331	110.3	44
	>100	0	295	$\infty$	39

The scope of the present study for vertex finding is still very limited since we performed our analysis only on the reconstructed impact parameters  $b_r$  in  $r\phi$  projected plane and only for 500 GeV/c  $90^\circ$   $b\bar{b}$  events. Further reconstruction steps are need to be taken ( and not done in the present paper) to identify the secondary vertices based on the tracks that survived the  $b_r$  and  $p_T$  cuts. With the similar procedures, one can extend the analysis to three dimensional vertex reconstruction, which will provide probably much better S/N ratios as well as better finding efficiencies. On the other hand, an inclusion of remaining other QCD multi-jet processes will reduce the S/N ratio by a factor several.

## 9. CONCLUSIONS

A specific design of microvertex detector for the SSC has been tried to assess the situation based on the silicon microstrip detector technology. The rate(occupancy) problem can be solved by introducing extremely fine segmentation of detectors, which in turn requires highly integrated special readout electronics with enough radiation resistance.

A simple Monte Carlo simulation indicated that secondary vertex tagging is quite promising based on the impact parameter study, though the estimation of backgrounds is too limited to conclude it strongly at this stage.

There are quite many R&D items to be pursued. As far as silicon microstrip detectors concern,

1. readout electronics with parallel-in serial-out buffers,
2. radiation hardened electronics,
3. double sided microstrip detectors

are of high priority.

Further Monte Carlo simulations are also strongly recommended in order to verify (or deny) the possibility of secondary vertex tagging, since we believe that identification of high energy  $b$  or  $c$  quark jets or  $\tau$  leptons is one of the most important clues to understand expected-to-be extremely complicate events under the presence of extremely heavy backgrounds for new physics.

## References

1. Proceedings of the 1984 Summer Study on the Design and Utilization of the Superconducting Super Collider, Snowmass, pp.585-592.
2. Report of the Task Force on Detector R&D for the Superconducting Super Collider, SSC-SR-1021(1986) pp.44-60.
3. P.Shepard, in this proceedings.
4. J.T.Walker et al., Nucl. Instr. and Meth.226(84)200, C.Adolphsen et al., IEEE Trans. on Nucl. Science 33(86)57.
5. C.Adolphsen et al., SLAC-PUB-3924 (1986).
6. For examples, NA32, WA75 at CERN, E653, E691 at Fermilab.
7. Proceedings of 1984 Snowmass Study, pp.697-701. Report of the Task Force on Detector R&D for the SSC, pp.208-219. D.Hartill, IEEE Trans. Nucl. Science 33(86)36.
8. E.H.Heijne, CERN 83-06(1983). P.Borgeaud et al., Nucl. Instr. and Meth.211(83)363. T.Kondo et al., Proceedings of 1984 Snowmass Study, p. 612.
9. R.Ruchti et al., IEEE Trans. Nucl. Science 33(86)151. A.E.Baumbaugh et al., IEEE Trans. Nucl. Science 33(86)903.
10. A.D.Bross, IEEE Trans. Nucl. Science 33(86)144.
11. P.Rehak et al., Nucl. Instr. and Meth. A235(85)224.
12. R.Bouclier et al., IEEE Trans. Nucl. Science 33(86)169.
13. Report of the Task Force on Detector R&D for the Superconducting Super Collider, SSC-SR-1021(1986) pp.61-71.
14. H.Anders et al., CERN/EF 85-10(1985).